Author(s): Lindén, J. & Hietaniemi, J. & Ikonen, E. & Lippmaa, M. & Tittonen, I. & Katila, T. & Karlemo, T. & Karppinen, Maarit & Niinistö, L. & Ullakko, K.

Title: Europium-based high-temperature superconductors studied by x-ray diffraction and 151Eu Mössbauer spectroscopy

Year: 1992

Version: Final published version

Please cite the original version:

Lindén, J. & Hietaniemi, J. & Ikonen, E. & Lippmaa, M. & Tittonen, I. & Katila, T. & Karlemo, T. & Karppinen, Maarit & Niinistö, L. & Ullakko, K. 1992. Europium-based high-temperature superconductors studied by x-ray diffraction and 151Eu Mössbauer spectroscopy. Physical Review B. Volume 46, Issue 13. 8534-8541. ISSN 1550-235X (electronic). DOI: 10.1103/physrevb.46.8534.

Europium-based high-temperature superconductors studied by x-ray diffraction and ^{151}Eu Mössbauer spectroscopy

J. Lindén, J. Hietaniemi, E. Ikonen,* M. Lippmaa, I. Tittonen, and T. Katila
Department of Technical Physics, Helsinki University of Technology, SF-02150 Espoo, Finland

T. Karlemo, M. Karppinen, and L. Niinistö
Laboratory of Inorganic and Analytical Chemistry, Helsinki University of Technology, SF-02150 Espoo, Finland

K. Ullakko
Laboratory of Engineering Materials, Helsinki University of Technology, SF-02150 Espoo, Finland
(Received 20 April 1992)

Isotropic powders and magnetically aligned crystallites of $EuBa_2Cu_3O_{7-\delta}$ (1:2:3) and europium-doped $Bi_2Sr_2CaCu_2O_8$ (2:2:1:2) were studied by means of x-ray diffraction and ^{151}Eu Mössbauer spectroscopy. The degree of crystallite orientation of the samples and the values of the lattice constants were determined by x-ray diffraction. The Mössbauer spectra were analyzed considering the full hyperfine Hamiltonian of the nuclear states of the 21.5-keV γ transition. The Mössbauer hyperfine parameters obtained from the superconducting and semiconducting phases are presented. A small change is seen in the ^{151}Eu isomer shift when the oxygen deficiency δ of the 1:2:3 compound is varied. The shift can be explained by a decrease in the *s*-electron density due to lattice expansion. The changes in the oxidation state of the copper atoms with varying δ were determined from the Mössbauer data: The Cu(2) atoms retain their oxidation state, whereas the Cu(1) atoms adjust their valence according to the value of δ. In the 2:2:1:2 samples, the Eu concentration clearly affected the value of the electric-field gradient at the Eu nucleus. Using a standard procedure, magnetically aligned 2:2:1:2 samples were prepared. The preferred direction of the crystal *c* axis changed from parallel to perpendicular alignment with the external magnetic field, when the Eu concentration exceeded 20% of the Ca atoms.

I. INTRODUCTION

The existence of antiferromagnetic and superconducting parent phases in the ceramical cuprates is important for the mechanisms of superconductivity, due to the mutually exclusive characters of these phases. In the so-called 1:2:3 compounds, superconductivity is depressed in favor of antiferromagnetism by simply removing oxygen atoms from the crystal lattice. In other compounds, depression of superconductivity is achieved by cationic substitution. The critical temperature T_c depends mainly on the hole concentration, which is usually associated with the formal valence of copper. Therefore knowledge of the oxidation state of copper is of crucial interest. This motivates a thorough characterization of a wide range of samples between the two extremes of superconductivity and semiconductivity.

Due to the anisotropic magnetic susceptibility, powders of high-T_c samples exhibit orientational effects in strong magnetic fields. In most compounds the *c* axis aligns parallel with the external magnetic field.[1,2] If, however, the compound contains some amount of europium the *c* axis will orient perpendicularly to the field. This is probably due to the large magnetic moment of the Eu atoms, the preferred direction of which is in a plane perpendicular to the *c* axis.

In the $Bi_2Sr_2(Ca_{1-y}Eu_y)Cu_2O_{8+\epsilon}$ system, europium or other rare-earth elements play the role of a cationic dopant. Europium-substituted samples are superconducting up to $y=0.6$. If higher concentrations are used the samples obtained are semiconducting. Doping with europium promotes the intercalation of excessive oxygen (ϵ) into the structure, probably at the BiO layer. An increase of the *a* and *b* lattice parameters and a decrease of the *c* lattice parameter results.[3] The Eu doping also reduces the formation of impurity phases, which is of importance because of the difficulty to prepare single-phase materials. Previous results indicate that highly doped samples exhibit antiferromagnetic ordering.[4–6]

The ^{151}Eu resonance has successfully been used for determination of the hyperfine parameters of the rare-earth site in the $EuBa_2Cu_3O_{7-\delta}$ superconductor.[7–11] The observed line broadening is explained by an electric quadrupole interaction at the europium nucleus, which splits the resonance into 12 unresolved lines.[9–11] Four lines correspond to usually forbidden transitions and have low intensities even when the spin states exhibit maximum mixing. The interaction depends solely on the principal component V_{zz} and the asymmetry parameter η of the electric-field-gradient tensor. The set of spectral components is therefore a rather well fixed entity, which enables reliable fitting of seemingly featureless spectra. There is a common agreement about the negative sign of V_{zz}, contrary to the predictions of simple point-charge calculations.[9–12] An earlier ^{151}Eu Mössbauer study on the $Bi_2Sr_2EuCu_2O_{8+\epsilon}$ sample has been reported.[13] The

Mössbauer spectra obtained are similar to those of 1:2:3 samples. This is due to the fact that the nearest neighbors of the rare-earth element are almost the same in both compounds.

In this work we study the hyperfine interactions at the rare-earth site in samples of $Bi_2Sr_2(Ca_{1-y}Eu_y)Cu_2O_{8+\epsilon}$ and $EuBa_2(Cu_{1-x}{}^{57}Fe_x)_3O_{7+\delta}$ by means of ^{151}Eu Mössbauer spectroscopy. The results indicate that a low iron doping ($x=0.01$, 0.02) does not affect the data obtained with the ^{151}Eu resonance. The lattice parameters were measured by x-ray diffractometry. It is shown that the value of V_{zz} together with point-charge calculations can be used to determine changes in the oxidation state of copper in 1:2:3 materials. A change in the isomer shift related to the unit-cell volume is also observed. A trial was made to observe antiferromagnetic ordering in the $Bi_2Sr_2EuCu_2O_{8+\epsilon}$ compound at 100 K.

II. EXPERIMENT

The preparation of the $EuBa_2(Cu_{1-x}{}^{57}Fe_x)_3O_{7-\delta}$ samples was as follows.[14] Stoichiometric quantities of Eu_2O_3, $BaCO_3$, CuO (99.99%), and ^{57}Fe (95% enriched) were carefully mixed in an agate mortar. The mixture was calcined in an Al_2O_3 crucible for 15 h at 950 °C in air. After grinding, the calcination was repeated. The desired oxygen deficiency was obtained by a heat treatment in an oxygen atmosphere at a temperature determined by the thermogravimetric data given in Ref. 14. The iron atoms ($x=0.00,\ldots,0.02$) were added to enable measurements with the ^{57}Fe Mössbauer resonance.[11,14] Several samples with the oxygen deficiencies of $\delta=0.1$, 0.5, and 0.8 were prepared and measured with the ^{151}Eu resonance. Additionally, we synthesized one batch of samples having oxygen deficiencies $\delta=0.1$, $0.2,\ldots,0.8$ for x-ray and Mössbauer measurements. However, the $\delta=0.8$ sample obtained consisted of several phases and could not be used.

The Eu-doped 2:2:1:2 samples were synthesized by a solid-state reaction of Bi_2O_3, $SrCO_3$, $CaCO_3$, CuO, and Eu_2O_3 (99.99%) as starting materials. The powders were carefully mixed and calcined in Al_2O_3 crucibles at 840 °C in air. Subsequent annealings at 850, 860, and 870 °C were followed by grinding.

The samples were encapsulated in small acrylic containers for Mössbauer measurements. The powders were mixed with an inert plastic compound to ensure homogeneity and formed a thin layer with a powder surface density of 22 mg/cm^2. Magnetically oriented 2:2:1:2 samples were made by subjecting the containers to a magnetic field of 11.7 T. The powders were soaked in epoxy resin and left to harden in the field. The samples with Eu contents $y=0.2$, 0.6, and 1.0 were oriented in two different geometries, with the magnetic field either parallel with or perpendicular to the intended direction of the γ beam. The rest of the 2:2:1:2 samples were oriented only in the parallel geometry.

Mössbauer measurements were performed in transmission geometry at room temperature and at 100 K for the $y=1.0$ sample. A 100-mCi ^{151}Sm:Sm_2O_3 source was used. The maximum Doppler velocity was usually between 2.5 and 10.0 mm/s. Velocities up to 20 mm/s were used for searching traces of europium in the 2+ oxidation state. The x-ray studies were performed using the Co $K\alpha_1$ radiation. We used a Siemens diffractometer equipped with an instrumentation électronique curved position sensitive 120 detector. The 2θ axis was calibrated separately for every measurement by adding silicon powder to the sample. The x-ray patterns were fitted with a least-squares program using Pearsonian lines. The line intensities and the lattice parameters were free-fitting parameters.

III. RESULTS AND DISCUSSION

In all ^{151}Eu Mössbauer measurements, one broadened resonance line close to zero velocity was obtained. A single-line Lorentzian could not explain the data. Thus the spectra were analyzed using the full Hamiltonian of the excited $I'=\frac{7}{2}$ and ground $I=\frac{5}{2}$ spin states. Fitting parameters were V_{zz}, η, the isomer shift (S), the background counting level, and the total absorption. For the 1:2:3 compounds, each component line had the same width, which also was a fitting parameter. For the 2:2:1:2 samples, the linewidth was fixed according to the source linewidth and the thickness of the sample. The quadrupole moments of the excited and the ground state were fixed to $Q_e=1.50$ and $Q_g=1.14\times10^{-28}$ m^2, respectively.[15] In the analysis of the low-temperature measurements, a possible magnetic interaction was taken into account in the Hamiltonian. The calculation of the line positions and intensities for Mössbauer spectra in different sample geometries is presented in the Appendix. Results from measurements made on different samples corresponding to the same stoichiometry were in agreement within the statistical uncertainties and were therefore combined. In Fig. 1, a Mössbauer spectrum obtained from a 2:2:1:2 compound with $y=1$ is presented. The crystallites were aligned with the magnetic field perpendicular to the intended direction of the γ rays. In this case $\theta_0=0$ according to the notation in the Appendix.

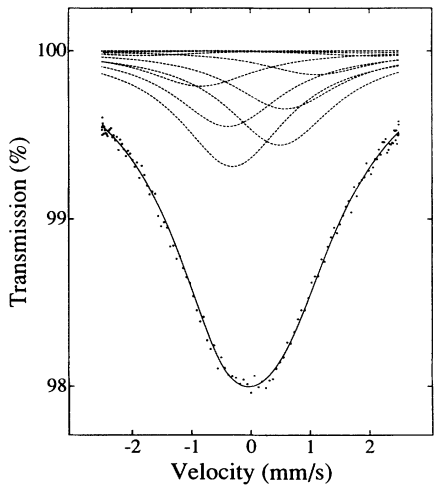

FIG. 1. Mössbauer spectrum of the magnetically oriented $Bi_2Sr_2EuCu_2O_{8+\epsilon}$ sample measured at room temperature. The 12 components used in the fit are indicated.

A. $EuBa_2(Cu_{1-x}{}^{57}Fe_x)_3O_{7-\delta}$ samples

The values of the lattice parameters in 1:2:3 compounds were measured by means of x-ray diffractometry. When changing the oxygen deficiency from 0.1 to 0.7, the unit-cell volume increased from 178.2 to 181.7 Å^3 (Fig. 2). The transition from orthorhombic to tetragonal structure took place at $\delta \simeq 0.6$.

A clear correlation between the oxygen contents and the Mössbauer isomer shift S is observed.[11] The measured isomer shifts, relative to the ^{151}Sm:Sm_2O_3 source, varied between 0.051(3) mm/s ($\delta=0.1$) and 0.011(3) mm/s ($\delta=0.8$), giving a difference in the isomer shift of $\Delta S=0.040(4)$ mm/s. The results of these measurements are shown in Fig. 3. For Eu^{3+}, the following experimental dependence between changes in the s-electron density $\Delta\rho$ and the unit-cell volume ΔV has been reported:[16]

$$\Delta\rho = -5.43 a_0^{-3} \Delta V/V \ , \tag{1}$$

where a_0 is the Bohr radius. The dependence between the s-electron density and the isomer shift is given in Ref. 17 as

$$\Delta S = \beta_i \Delta\rho \Delta\langle R^2\rangle \ , \tag{2}$$

where $\Delta\langle R^2\rangle = 19.2\times10^{-3}$ fm^2 represents the change in the nuclear radius during the γ transition and the proportionality constant is $\beta_i = 17.7 a_0^3$ fm^{-2} mm/s. By extracting $\Delta V/V$ from a linear regression of the data in Fig. 2 we may calculate ΔS using Eqs. (1) and (2). The slope of the measured data in Fig. 3 is remarkably well reproduced by the calculated curve, obtained without fitted parameters. The result above confirms that for any oxygen deficiency the electron configuration of the europium atom remains unchanged, except for a small expansion of the electron shells.

The parameters V_{zz} and η are presented in Figs. 4 and 5.[11] For the quadrupole coupling constant eQ_gV_{zz} we obtained values between $-5.28(13)$ and $-5.89(11)$ mm/s, while the asymmetry parameter varied between 0.65(5) and 0.80(5). Because of the low iron concentrations, no differences were seen between the parameter values for pure and iron-doped 1:2:3 compounds.

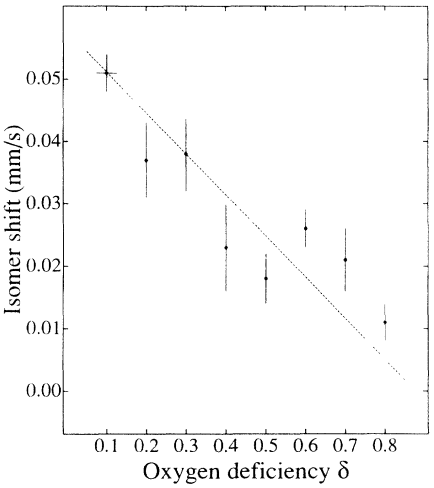

FIG. 3. Measured and calculated ^{151}Eu isomer shifts as a function of the oxygen deficiency δ for the $EuBa_2(Cu_{1-x}{}^{57}Fe_x)_3O_{7-\delta}$ samples. The dashed line is deduced from the unit-cell-volume data of Fig. 2 using the procedure explained in the text.

We simulated the behavior of V_{zz} using point-charge calculations. The calculations of V_{zz} give only the lattice contribution (lat), while the portion caused by the valence electrons (val) of the Eu atom remains unknown. The valence part should, however, be almost constant for samples differing only little in structure and stoichiometry. The behavior of the isomer shift supports this assumption. We use the conventional decomposition of V_{zz}:[18]

$$V_{zz} = (1-\gamma_\infty)V_{zz}^{\rm lat} + (1-\sigma)V_{zz}^{\rm val} \ , \tag{3}$$

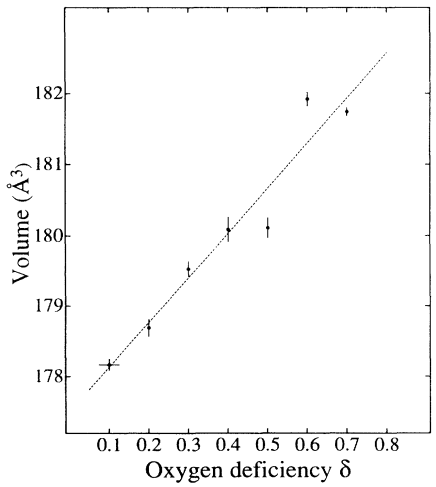

FIG. 2. Unit-cell volume of the $EuBa_2(Cu_{1-x}{}^{57}Fe_x)_3O_{7-\delta}$ samples as a function of δ. The dashed line is a linear fit to the data.

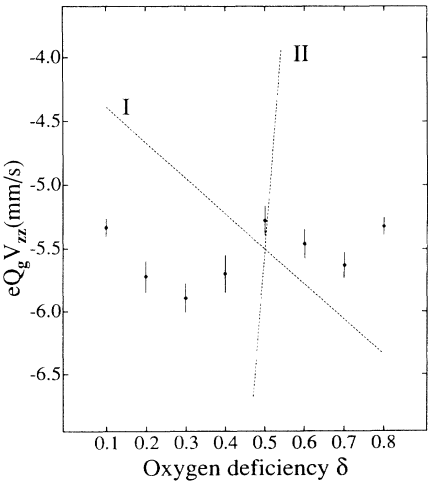

FIG. 4. Measured values of the main component of the electric-field gradient eQ_gV_{zz}. The dashed lines are calculated results by hypotheses I and II (see text).

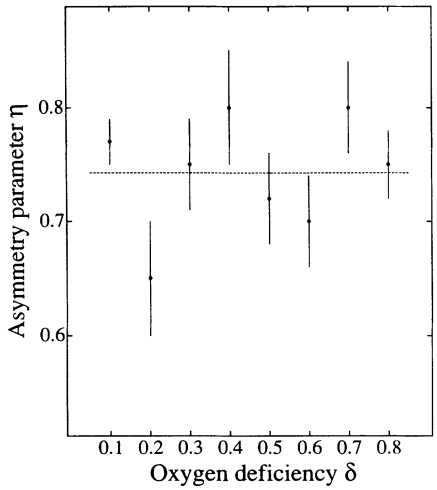

FIG. 5. Measured values of the asymmetry parameter η. The average value $\bar{\eta}=0.74$ is indicated by the dashed line.

where γ_∞ and σ are the lattice and valence terms of the Sternheimer shielding factors, arising from the inner electron shells of the atom. The following values were used: $\gamma_\infty=-87$ and $\sigma=0.73$.[19] These values are typical of rare-earth ions in a 3+ oxidation state,[20,21] and they are expected to apply to the present compounds.

We used measured values of the lattice parameters and coordinates of the atoms for $0\leq\delta\leq1$.[22,23] The amount of oxygen vacancies along the Cu(1) chains was determined by δ, and the vacancies were supposed to be randomly distributed. The charge neutrality was retained using two different hypotheses: adjustment of the valence of either (I) the Cu(1) atoms or (II) the Cu(2) atoms. According to hypothesis I, the Cu(1) valence varies between 1+ and 3+ as δ changes from 1.0 to 0.0, and the Cu(2) valence is 2+. In case II, the Cu(1) valence is fixed to 2+, while the Cu(2) valence varies between 1.5+ and 2.5+. When $\delta=0.5$ both hypotheses give the same values for the valence of the copper atoms. In calculating $V_{zz}^{\rm lat}$ the direction of the z axis was taken parallel to the crystal c axis, an assumption supported also by Ref. 10. Both of our hypotheses yielded positive values of $V_{zz}^{\rm lat}$ in agreement with other point-charge calculations and contrary to the experimental data.[9–12] The simulated values were, however, used only to evaluate the dependence of V_{zz} on δ.

It turned out that hypothesis I results in a weak linear dependence between $V_{zz}^{\rm lat}$ and δ: $V_{zz}^{\rm lat}=0.23\times10^{21}$ V/m^2 ($\delta=0$) and $V_{zz}^{\rm lat}=0.21\times10^{21}$ V/m^2 ($\delta=1$). Hypothesis II gave a strong linear dependence: $V_{zz}^{\rm lat}=0.08\times10^{21}$ V/m^2 ($\delta=0$) and $V_{zz}^{\rm lat}=0.36\times10^{21}$ V/m^2 ($\delta=1$).

For $\delta=0.5$ we obtain an average value $V_{zz}^{\rm lat}=0.22\times10^{21}$ V/m^2 corresponding to $(1-\gamma_\infty)eQ_gV_z^{\rm lat}=30.7$ mm/s in velocity units. With the experimental result $eQ_gV_{zz}=-5.5$ mm/s we get by Eq. (3), $(1-\sigma)eQ_gV_{zz}^{\rm val}=-36.2$ mm/s. Using this calculated value for $eQ_gV_{zz}^{\rm val}$, which may be taken as a constant for the whole range of δ, and the lattice contributions from the point-charge calculations, we may evaluate eQ_gV_{zz} as a function of δ. The results for both hypotheses are shown in Fig. 4. In view of this picture, hypothesis II has to be rejected, whereas hypothesis I yields quite a consistent description of V_{zz}. The fine structure in the V_{zz} data, if any, could not be explained within the framework of this model.

B. $Bi_2Sr_2(Ca_{1-y}Eu_y)Cu_2O_{8+\epsilon}$ samples

The lattice parameters a,b,c and the unit-cell volume of the 2:2:1:2 samples are shown as a function of y in Figs. 6 and 7. The statistical error estimates are less than the size of the symbols used and remeasurements of some samples reproduced the results within the statistical error. The a and b parameters increase from 5.3987(4) to 5.4705(1) and from 5.426(1) to 5.5017(2), respectively, when y increases from 0.0 to 1.0, while the c parameter decreases from 30.759(1) to 30.333(1) in the same y range. The deviation in the c parameter at $y=0.6$ may be an erratic result due to the chemical synthetization procedure. The unit-cell volume is close to 902 Å^3 between $y=0.0$ and 0.8 and reaches its maximum value of 912.9(2) Å^3 at $y=1.0$. The above behavior is in accordance with results obtained by neutron diffraction.[3]

Because of the large magnetic moment of the Eu atom, the europium doping affects the direction in which the crystallites align, when the samples are subjected to strong magnetic fields. If the Eu percentage is low (in our case $y\leq0.2$) the c axes of the crystallites orient parallel with the field but perpendicular to it when y acquires higher values ($y\geq0.25$). This is illustrated in Fig. 8. The first two x-ray patterns [(a) and (b)] were measured on the $y=0.2$ sample oriented with the field perpendicular to the surface of the sample (a) and the field parallel to the sample surface (b). The third pattern (c) was obtained for the $y=0.25$ sample oriented with the field perpendicular to the surface of the sample. The similarity of patterns (b) and (c) supports the conclusions presented above.

The dependence between the hyperfine parameters and

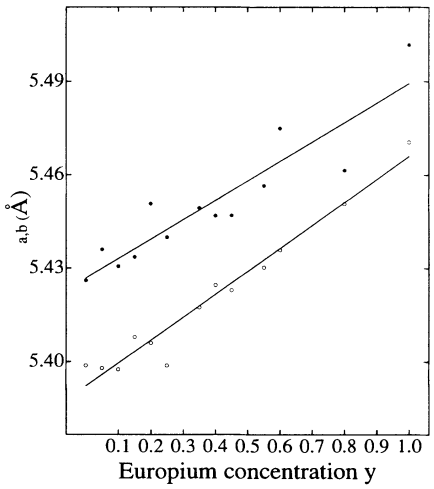

FIG. 6. Unit cell parameters a (○) and b (●) as a function of the Eu contents y in the $Bi_2Sr_2(Ca_{1-y}Eu_y)Cu_2O_{8+\epsilon}$ samples. The straight lines are linear fits to the data.

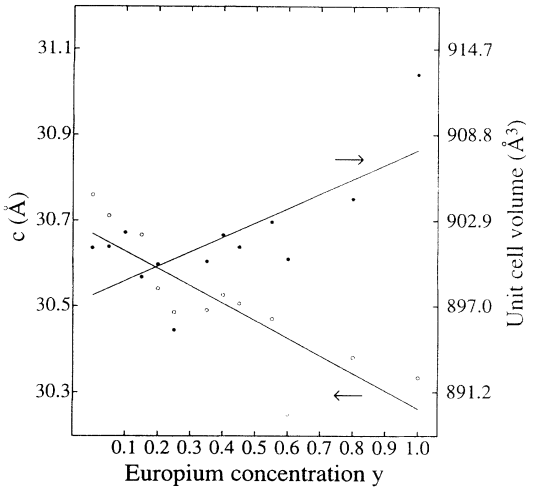

FIG. 7. Lattice parameter c (○) and the unit-cell volume (●) as a function of the Eu contents y in the $Bi_2Sr_2(Ca_{1-y}Eu_y)Cu_2O_{8+\epsilon}$ samples. The straight lines are linear fits to the data.

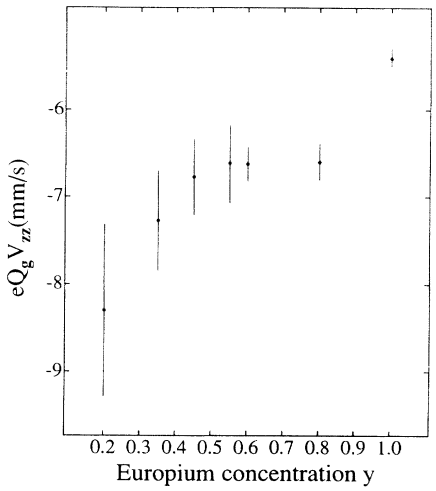

FIG. 9. Main component of the electric-field gradient eQ_gV_{zz} of the $Bi_2Sr_2(Ca_{1-y}Eu_y)Cu_2O_{8+\epsilon}$ samples as a function of Eu contents y.

the europium concentration was difficult to extract due to the low resonance absorption, especially in the lightly doped samples. The values of the hyperfine parameters are shown in Figs. 9–11. The value of eQ_gV_{zz} increased from $-8.3(1.0)$ mm/s ($y=0.2$) to $-5.40(12)$ mm/s ($y=1.0$), which can be explained by intercalation of excess oxygen. The asymmetry parameter η was close to 0.4, except for the $y=1.0$ sample, for which $\eta=0.87(4)$. From a linear regression of the volume data in Fig. 7 we calculated the isomer shift using Eq. (1) and (2). The result is presented by the dashed line in Fig. 11. The isomer shift was practically constant within the statistical error limits. Such a behavior is expected since x-ray diffractometry indicates a low expansion of the lattice. The average value $S=0.03$ mm/s verifies that the europium ions adopt the 3+ oxidation state, contrary to the 2+ state of calcium. No traces of Eu^{2+} were found in measurements performed with a maximum velocity of 15 mm/s. Apart from forcing excess oxygen into the lattice, europium lowers the formal valence of copper.[24]

Mössbauer spectra of oriented samples exhibited an asymmetry in the resonance line due to the changes in the intensities of the nuclear transitions as compared to isotropic samples. Computer fitting of Mössbauer spectra using the formalism given in the Appendix supported the assumption that when $y \leq 0.2$ the crystallites orient with the c axis parallel with the magnetic field, while higher Eu percentages (in our Mössbauer measurements $y=0.6$ and 1.0) cause the crystallites to orient perpendicular to the field.

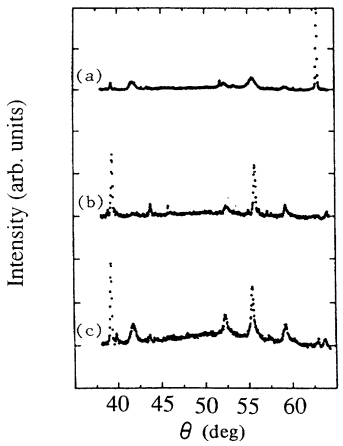

FIG. 8. X-ray diffraction patterns for oriented $Bi_2Sr_2(Ca_{1-y}Eu_y)Cu_2O_{8+\epsilon}$ samples with $y=0.2$ [(a) and (b)] and $y=0.25$ (c). The samples were oriented with the magnetic field perpendicular to [(a) and (c)] or parallel with (b) the surface of the sample.

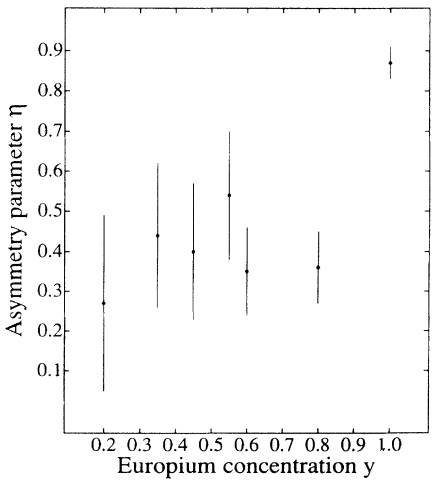

FIG. 10. Asymmetry parameter η of the $Bi_2Sr_2(Ca_{1-y}Eu_y)Cu_2O_{8+\epsilon}$ samples as a function of the Eu contents y.

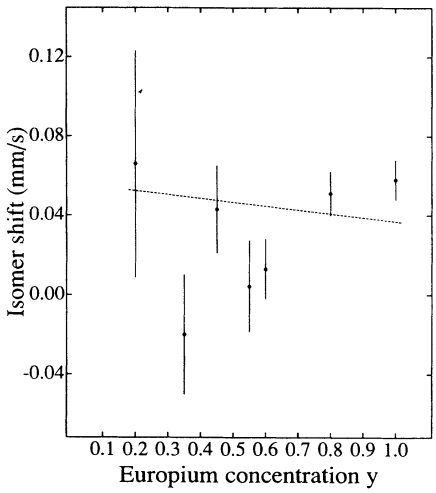

FIG. 11. Isomer shift as a function of the Eu contents y for the $Bi_2Sr_2(Ca_{1-y}Eu_y)Cu_2O_{8+\epsilon}$ samples. The dashed line is deduced from the unit-cell-volume data of Fig. 7 using the procedure explained in the text.

In the measurement of the $Bi_2Sr_2EuCu_2O_{8+\epsilon}$ sample at 100 K, no conclusive answer was found to the question whether there is a magnetic field at the Cu nucleus. Since the magnetic moment of the Eu atom seems to be perpendicular to the c axis, a magnetic field ($\mathbf{B}_{\text{eff}}$) was included into the Hamiltonian as a term perpendicular to the quantization axis defined by V_{zz}. The magnetic-field strength at the nucleus was found to be less than 0.4 T. When attempting to fit the spectrum with $\mathbf{B}_{\text{eff}}$ parallel to V_{zz}, the value obtained was 0 T within the error estimate.

IV. CONCLUSIONS

In this work the hyperfine parameters at the rare-earth site in $EuBa_2Cu_3O_{7-\delta}$ and Eu-doped $Bi_2Sr_2CaCu_2O_8$ superconductors were studied. The full quadrupole Hamiltonian was successfully applied in analyzing the measured Mössbauer spectra. The isomer shift obtained for the 1:2:3 samples correlates with changes in the unit-cell volume, induced by the oxygen deficiency. The value of the electric-field gradient at the rare-earth site in these compounds reflects the stability of the oxidation state of the Cu(2) atoms. We may therefore conclude that the changes in the oxidation state of copper take place at the Cu(1) site. A 2% replacement of the copper atoms with iron does not affect the parameters obtained with the ^{151}Eu resonance.

The previously reported increases in the a and b lattice parameters and decreases in the c lattice parameter as a function of the Cu concentration in 2:2:1:2 samples were confirmed. The Eu concentration clearly affected the value of V_{zz}, probably due to the excessive oxygen entering the lattice. The orientation of the crystal c axis in a 11.7-T magnetic field was found to be dependent on the Eu contents, with a critical value between $y=0.2$ and $y=0.25$. In the 100-K spectra of nonsuperconducting 2:2:1:2 samples, a possible magnetic field at the europium site was found to be less than 0.4 T.

ACKNOWLEDGMENTS

Financial support from the following foundations is gratefully acknowledged: Tekniska föreningen i Finland (J. L.), Emil Aaltonen Foundation (J. L. and I. T.), and Wihuri Foundation (I. T. and M. L.). The Institute of Chemical Physics and Biophysics at the Estonian Academy of Sciences is acknowledged for providing the magnet in the orienting experiments.

APPENDIX

In this appendix the line intensities and positions of the 21.5-keV $M1$ transition of ^{151}Eu are analyzed. The Hamiltonian describing the hyperfine interactions at the europium nucleus is[18]

$$\mathcal{H}=\frac{eQV_{zz}}{4I(2I-1)}\left[3\hat{I}_z^2-\hat{I}^2+\frac{\eta}{2}(\hat{I}_+^2+\hat{I}_-^2)\right]-\boldsymbol{\mu}\cdot\mathbf{B}_{\text{eff}}\ , \tag{A1}$$

where $\hat{I},\hat{I}_z,\hat{I}_\pm$ are spin operators ($\hat{I}_\pm=\hat{I}_x\pm i\hat{I}_y$), Q and $\boldsymbol{\mu}$ are the quadrupole moment and the magnetic dipole moment of the nucleus, respectively. A magnetic interaction $\boldsymbol{\mu}\cdot\mathbf{B}_{\text{eff}}$ is added to the Hamiltonian. If $\mathbf{B}_{\text{eff}}$ is not parallel with the quantization axis determined by V_{zz}, the proper rotation matrix is applied to the magnetic part of the Hamiltonian. The excited-state spin is $I'=\frac{7}{2}$ and the ground-state spin is $I=\frac{5}{2}$. Therefore in the $|I',m'\rangle$ and $|I,m\rangle$ bases Eq. (A1) corresponds to 8×8 and 6×6 matrices, respectively. For an $M1$ transition this gives in principle $(2I'+1)\times(2I+1)$ lines. If, however, the magnetic interaction is zero all the spin states exhibit at least a twofold degeneration, producing the 12 lines used in our room-temperature fittings. The line positions are found by diagonalizing the matrices and calculating the differences between the energy eigenvalues. The line intensities are obtained from the proper Clebsch-Gordan coefficients, rotation-matrix elements, and the expansion coefficients $a_{m'}^{(n')}$ and $b_m^{(n)}$ of the diagonalized excited ($|\Phi_{n'}\rangle$) and ground ($|\Phi_n\rangle$) eigenvectors

$$|\Phi_{n'}\rangle=\sum_{m'=-7/2}^{7/2}a_{m'}^{(n')}|I',m'\rangle$$

and (A2)

$$|\Phi_n\rangle=\sum_{m=-5/2}^{5/2}b_m^{(n)}|I,m\rangle\ .$$

The amplitudes of γ transitions between the states labeled by n and n' are proportional to the matrix element of the Hamiltonian $\mathcal{H}'$ describing the interaction between the nucleus and the γ quanta:

$$v_{n'n}=\langle\Phi_{n'},\chi(0)|\mathcal{H}'|\Phi_n,\chi(\mathbf{k}p)\rangle\ , \tag{A3}$$

where $\chi(0)$ and $\chi(\mathbf{k}p)$ are the photon vacuum state and a photon state with a momentum $\mathbf{k}$ and left-handed ($p=+1$), or right-handed ($p=-1$) polarization. Following the formalism of Blume and Kistner,[25] the matrix element (A3) is simplified to enable numerical calculations. Omitting the normalization factors we obtain

$$v_{n'n}(p,\theta,\phi)=\sum_{m'm} a_{m'}^{(n')*} b_m^{(n)} D^{(1)}_{m'-m,p}(\phi\theta 0) \times C(\tfrac{7}{2},1,\tfrac{5}{2};m',m'-m,m) \ . \quad \text{(A4)}$$

The angle between the photon direction and the quantization axis is denoted by polar angle θ, while the corresponding azimuthal angle is given by ϕ. The Clebsch-Gordan coefficients between the pure $\frac{7}{2}$ and $\frac{5}{2}$ spin states and the spin-1 rotation matrix of the $M1$ transition are denoted by $C(\frac{7}{2},1,\frac{5}{2};m',m'-m,m)$ and $D^{(1)}_{m'-m,p}(\phi\theta 0)$, respectively. The normalized transition probability,

$$P_{n'n}=|v_{n'n}(+1,\theta,\phi)|^2+|v_{n'n}(-1,\theta,\phi)|^2 \ , \quad \text{(A5)}$$

directly gives the line intensities when using a single-line source.

When using an isotropic powder absorber, the transition probability should be averaged over a 4π solid angle. Upon integrating (A5), the rotation-matrix factors yield simply a Kronecker-δ term. Hence, for an isotropic absorber we obtain

$$P_{n',n}=\sum_{m',ml',l} a_{m'}^{(n')} a_{l'}^{(n')*} b_m^{(n)*} b_l^{(n)} C(\tfrac{7}{2},1,\tfrac{5}{2},m',m'-m,m) \times C(\tfrac{7}{2},1,\tfrac{5}{2},l',l'-l,l)\delta_{m'-m,l'-1} \ . \quad \text{(A6)}$$

When the absorber consists of oriented crystallites two different cases arise. If the c axis aligns with the magnetic field, θ remains well defined. If however, the c axis orients perpendicularly to the magnetic field, it is the normal to the plane in which the c axes lie, which constitutes a well-defined direction. The angle between the normal and the direction of the photon is denoted by $90°-\theta_0$. In either case ϕ remains arbitrary and averaging of ϕ over 2π is therefore required, a process yielding a Kronecker-δ factor and a θ-dependent term, denoted by $d_{l'-l,\pm 1}(\theta)$:

$$P_{n',n}=\sum_{m',m,l',l} a_{m'}^{(n')} a_{l'}^{(n')*} b_m^{(n)*} b_l^{(n)} C(\tfrac{7}{2},1,\tfrac{5}{2},m',m'-m,m) C(\tfrac{7}{2},1,\tfrac{5}{2},l',l'-l,l) \times [d_{m'-m,1}(\theta) d^*_{l'-l,1}(\theta)+d_{m'-m,-1}(\theta) d^*_{l'-l,-1}(\theta)]\delta_{m'-m,l'-l} \ . \quad \text{(A7)}$$

The θ-dependent part of Eq. (A7) is

$$|d_{\pm 1,+1}(\theta)|^2+|d_{\pm 1,-1}(\theta)|^2=\tfrac{1}{4}+\tfrac{1}{4}\cos^2\theta$$

and (A8)

$$|d_{0+1}(\theta)|^2+|d_{0,-1}(\theta)|^2=\tfrac{1}{2}\sin^2\theta \ .$$

In the so-called magic angle ($\theta\simeq 54.74°$) the intensities coincide with those obtained for isotropic absorbers, which is seen when the polar angles in Eq. (A8) are averaged over π. In the case when the c axes lie in the plane perpendicular to the magnetic field, the θ-dependent part must be averaged over a suitable geometry, defined by θ_0. We may therefore express θ as

$$\cos\theta=\cos\theta_0\cos\phi_p \ , \quad \text{(A9)}$$

where ϕ_p gives the direction of an arbitrary c axis in a plane perpendicular to the external magnetic field. The transition probabilities are obtained by inserting Eq. (A9) in (A8) and averaging ϕ_p from 0 to $\pi/2$, keeping θ between 0 and $\pi/2$. Note that the intensities of an isotropic absorber are in this case obtained for $\theta_0=35.26°$.

*Present address: Metrology Research Institute, Helsinki University of Technology.

[1]J. M. Ferreira, M. B. Maple. H. Zou, R. R. Hake, B. W. Lee, C. L. Seaman, M. V. Kuric, and R. P. Guertin, Appl. Phys. A **47**, 105 (1988).

[2]D. E. Farrell, B. S. Chandrasekhar, M. D. De Guire, M. M. Fang, V. G. Kogan, J. R. Clem, and D. K. Finnemore, Phys. Rev. B **36**, 4025 (1987).

[3]O. K. Antson, T. T. Karlemo, M. J. Karppinen, and K. Ullakko, Physica C **173**, 65 (1991).

[4]N. Nishida, S. Okuma, H. Miyatake, T. Tamegai, Y. Iye, R. Yoshizaki, K. Nishiyama, K. Nagamine, R. Kadono, and J. H. Brewer, Physica C **168**, 23 (1990).

[5]R. de Renzi, C. Bucci, P. Carretta, G. Guidi, R. Tedeschi, G. Calestani, and S. F. J. Cox, Physica C **162-164**, 155 (1989).

[6]Y. Akira, A. Jun, M. Hideaki, O. Satoshi, and N. Nobuhiko, J. Phys. Soc. Jpn. **59**, 1921 (1990).

[7]A. Freimuth, S. Blumenröder, G. Jackel, H. Kierspel, J. Langen, G. Buth, A. Nowack, H. Schmidt, W. Schlabitz, E. Zirngiebl, and E. Mörsen, Z. Phys. B **68**, 433 (1987).

[8]G. Wortmann, S. Blumenröder, A. Freimuth, and D. Riegel, Phys. Lett. A **126**, 434 (1988).

[9]Z. M. Stadnik. G. Stroink, and R. A. Dunlap, Phys. Rev. B **39**, 9108 (1989).

[10]M. Lippmaa, E. Realo, and K. Realo, Phys. Lett. A **139**, 353 (1989).

[11]I. Tittonen, J. Hietaniemi, J. Huttunen, E. Ikonen, M. Karppinen, T. Katila, J. Lindén, and L. Niinistö, Hyperfine Interact **55**, 1399 (1990).

[12]F. J. Adrian, Phys. Rev. B **38**, 2426 (1988).

[13]W. A. Groen, R. Steens, H. W. Zanderbergen, M. W. Dirken, F. M. Mulder, and R. C. Thiel, J. Less-Common Met. **155**, 133 (1989).

[14]E. Ikonen, J. Hietaniemi, K. Härkönen, M. Karppinen, T. Katila, J. Lindén, L. Niinistö, H. Sipola, I. Tittonen, and K. Ullakko, in *High-T_c Superconductors,* edited by H. W. Weber (Plenum, New York, 1988), p. 209.

[15]J. G. Stevens, in *Handbook of Spectroscopy,* edited by J. W. Robinson (CRC, Boca Raton, 1981), p. 468.

[16]G. M. Kalvius, U. F. Klein, and G. Wortmann, J. Phys. C **6**,

139 (1974).
[17]G. K. Shenoy and B. D. Dunlap, in *Handbook of Spectroscopy* (Ref. 15), p. 490.
[18]P. Gütlich, in *Topics in Applied Physics 5, Mössbauer Spectroscopy,* edited by U. Gonser (Springer, Berlin, 1975), p. 62.
[19]S. Bhattacharyya and D. Ghosh J. Magn. Magn. Mater. **80**, 276 (1989).
[20]R. M. Sternheimer, Phys. Rev. **132**, 1637 (1963).
[21]J. Blok and D. A. Shirley, Phys. Rev. **143**, 278 (1966).
[22]P. Meuffels, B. Rupp, and E. Pörschke, Physica C **156**, 441 (1988).
[23]A. Williams, G. H. Kwey, R. B. von Dreele, A. C. Larson, I. D. Raistrick, and D. L. Bisch, Phys. Rev. B **37**, 7960 (1988).
[24]M. Karppinen, O. Antson, P. Baulés, T. Karlemo, T. Katila, J. Lindén, M. Lippmaa, L. Niinistö, C. Roucau, I. Tittonen, and K. Ullakko, Supercond. Sci. Technol. (to be published).
[25]M. Blume and O. Kistner, Phys. Rev. **171**, 417 (1968).